Controlling the Resistivity of Multi-walled Carbon Nanotube Networks by Copper Encapsulation

Yong Sun*, Boateng Onwona-Agyeman, and Tatsuro Miyasato[1]

*Tel.: +81 93 884 3564; fax: +81 93 884 3560; sun@ele.kyutech.ac.jp

Department of Applied Science for Integrated System Engineering, Kyushu Institute of Technology, 1-1 Sensui-machi, Tobata, Kitakyushu-City, Fukuoka 804-8550, Japan

[1]Research and Development Center for Higher Education, Nagasaki University. 1-14 Bunkyou-Machi, Nagasaki-City, Nagasaki 852-5821, Japan

Abstract

The resistivity of multi-walled carbon nanotube networks can be *changed by filling Cu into the nanotubes as well as by preparing the nanotube networks with various densities.* The resistivity can be controlled to be lower than the c-axis resistivity of graphite, and has a low temperature coefficient of $-1.12 \times 10^{-5}/\mathrm{K}$ over the temperature range of $20\sim500$ K. *Filling Cu into the nanotubes decreases the intra-tube resistivity, but the temperature coefficient of the resistivity is governed by the inter-tube resistivity of the nanotube network.*

Keywords: multi-walled carbon nanotube network; copper encapsulation; electrical resistivity; temperature coefficient

1. Introduction

Carbon nanotubes (CNTs) are being used extensively for electronic applications such as in optoelectronic devices, transistors, touch-screens, flexible microelectronics, and chemical sensors [1]. In such applications, the CNTs are used in forms such as single tubes, bundles, random networks, and composites with polymers, metals, or ceramics. When CNTs are used in a device, foreign atoms will adsorb onto their internal and external surfaces, and this leads to degradation of their electronic properties of the device if the CNTs are single-walled carbon nanotubes (SWCNTs). For this reason, multi-walled carbon nanotubes (MWCNTs) are more suitable for the device applications than SWCNTs because the inner graphene walls of MWCNTs can remain unreacted and the essential electronic structures can be retained.

SWCNT films are attractive replacements for transparent conductors such as tin-doped indium oxide (ITO) and fluorine-doped tin oxide (FTO) in optoelectronic devices [2]. However, their room-temperature conductivity decreases by about four orders of magnitude as thickness decreases from 100 to 1 nm [3]. The resistance of the SWCNT films is dominated by the resistance of the intertube junctions formed from the crossed semiconducting SWCNTs. On the other hand, the electrical and optical properties of MWCNT films related to their thickness are still not studied in detail. *Moreover, it is highly possible to achieve low resistivity MWCNT films with reduced monolayer density by filling high-conducting metals into the MWCNTs resulting in a high transparency of MWCNT network as well.*

It is reported that the conductance of an individual MWCNT is lower than that of a SWCNT because the conductance is only formed at the outermost wall of the MWCNT and also, the interaction of the tube walls decreases the conductance. But recent results reveal a substantial contribution of conduction from the second wall after carriers tunnel from the outermost wall [4]. A perfect electrical contact with an MWCNT can be achieved by preparing the contact electrodes during the tube growth and this technique has shown that the conductivity of MWCNT can be several hundred times higher than that of SWCNT [5]. From the above results, new application fields based on MWCNT networks can be developed by controlling the contact properties of the MWCNTs with metals as well as by filling metals into the nanotubes.

In this study, we have prepared copper-filled MWCNT networks at various Cu concentrations, and the resistivity of the network prepared with various densities is measured as a function of temperature. Carrier transport mechanisms in the various networks are also discussed.

2. Experimental procedure

Laser vaporization of a carbon target containing Cu was carried out in an argon gas atmosphere at a pressure of 0.5 MPa. A continuous wave Nd:YAG laser was used to vaporize the Cu/carbon target at room temperature. The Cu-filled MWCNT (Cu@MWCNT) powders obtained were characterized by field emission scanning electron microscope (FE-SEM; JEOL JSM-7000), transmission electron microscope (TEM; HITACHI H-9000NAR), and X-ray diffraction (XRD; JEOL JDX-3500K). The compositions of C and Cu in the network are obtained by energy dispersive X-ray spectrometry (EDS) analysis during the SEM observation. The Cu@MWCNT powders were pressed into a pellet at room temperature and in vacuum at the pressures of 50, 76, 128, and 191 MPa for 30 min. The resultant pellets were 15 mm in diameter and 5 mm thick. Resistivity of the pellets was measured by means of four-point probe technique using a resistance tester (HIOKI 3541) with a resolution of 0.1 μΩ. The pellet was set in a chamber with a residual gas pressure of less than 10^{-5} Pa. The measurements were carried out in the temperature range of $20\sim500$ K in steps of 1 K during heating and cooling at a rate of $0.14\ \mathrm{K\ min^{-1}}$.

3. Results and discussion

The SEM image of a typical Cu@MWCNT pellet is shown in Fig. 1(a). The nanotubes with uniform diameter and high aspect-ratio, which constitute a random network, can be seen. *From the SEM image, it is suggested that the resistance of the network will be determined by the total resistance of the inter- and intra-tubes as the filling of copper changes only the resistance of the intra-tube.*

Figure 1(b) is a TEM image of the network showing filled and hollow tubes with an average diameter of about 20 nm as well as individual and large particles in the network. The analyses using electron beam diffraction showed that the hollow tube has the structure of graphite. The filled tube is Cu@MWCNT, and the large particles are rare Cu crystals, or are covered by graphite layer. The electron beam diffraction patterns of both a filled tube and a particle are shown in Figs. 1(c) and 1(d), respectively. For the filled tube in Fig. 1(c), the diffraction shows patterns from graphite (200) planes as well as the (111), (200), (220) and (311) planes of the face-centred cubic (fcc) Cu are observed. The result indicates that the filled tubes in the network are the MWCNTs filled by crystalline Cu. On the other hand, the diffraction spots from (111), (200), and (220) planes of copper show that the large particles in the network have a single-crystal Cu structure.

The Cu@MWCNT network of the pellet is also analyzed by X-ray diffraction. Diffraction patterns of the Cu@MWCNT powders exposed to air for one and nine weeks are shown in Fig. 2(a) and 2(b), respectively. Similar to the results obtained by the electron beam diffraction, the XRD patterns in Fig. 2 shows the diffractions from graphite (200) plane as well as from the (111), (200), and (220) planes of the fcc Cu as well as a diffraction peak from Cu_2O (111) planes. We found out that the intensity of the Cu_2O (111) peak depends on exposure time of the powders to air. The intensity ratios of the Cu_2O (111) peak to the Cu (111) peak are 0.10 and 0.18 for the exposure times of one and nine weeks. This suggests that the single-crystal Cu particles in the network are rare or are covered by a defective graphite layer.

The temperature dependences of the resistivities of the Cu-filled *and pristine* MWCNT network pellets prepared by applying pressure of 128 MPa are shown in Fig. 3 during the heating and cooling processes. The upper and bottom curves in the figure are related to the pellets with the C/Cu ratios of 0.73 and 0.57, respectively. The larger C/Cu ratio corresponds to a smaller filling yield of Cu into the tubes, and there is no significant difference on the dependences during the heating and cooling processes for the same pellet. The resistivity of the network decreases with increasing the Cu yield filled into the tubes. The resistivity is almost inversely proportional to the temperature with an average temperature coefficient of $-1.12 \times 10^{-5}/\mathrm{K}$ over the range of $20\sim500$ K. *On the other hand, the curves in the middle, corresponding to the scale of the right y-axis, show the temperature dependences of pristine MWCNT network during the heating and cooling processes. The pristine MWCNT network shows larger resistivity, about a hundred times that of the Cu@MWCNT network. But, the value of temperature coefficient is close to that of the Cu@MWCNT network, therefore, the temperature coefficient of the Cu@MWCNT network is governed by the inter-tube resistivity.*

The room-temperature resistivity of the Cu@MWCNT pellets with the C/Cu ratio of 0.57 is also measured for samples prepared at various pressures of 50, 76, 128, and 191 MPa. The room-temperature resistivity is shown in Fig. 4 as a function of pressure and it can be observed that resistivity decreases with increase in the applied pressure or the density of the network. Increasing the density of the Cu@MWCNT network is another means of effectively changing its resistivity apart from filling Cu into the tubes.

Based on the above results, we can discuss the mechanisms of carrier transport in the Cu@MWCNT network. Firstly, the resistivities of the Cu@MWCNT network at 300 K are 0.042 and 0.028 Ωcm for the C/Cu ration of 0.73 and 0.57. The values are lower than the resistivity (1 Ωcm [6]) of MWCNT film at 300 K, and are also lower than the c-axis resistivity (0.1 Ωcm [7]) of highly oriented pyrolytic graphite (HOPG) at 300 K. This indicates that the filling of Cu decreases effectively the resistivity of the MWCNT network.

Secondly, the measured temperature coefficient of the Cu@MWCNT networks has smaller value of $-1.12 \times 10^{-5}/\mathrm{K}$ over the temperature range of $20\sim500$ K. *This is due to the fact that the MWCNT has a negative temperature coefficient [6], and also as shown in Fig. 3. The result shows that, the filling of Cu can decrease the intra-tube resistivity of the Cu@MWCNT network.*

Thirdly, the contact resistance between the metal and MWCNT depends upon tunneling of electrons across a finite physical barrier created by Van der Waals interaction at the metal/CNT interface [8]. In this study, the barrier height depends mainly on the work function difference between Cu and MWCNT. The work functions are 4.8 eV for MWCNT [9], 4.48 eV for Cu(110), 4.53 eV for Cu(112), 4.59 eV for Cu(100), and 4.95 eV for Cu(111) surfaces [10]. The barrier leads to a contact resistance across the Cu/MWCNT interface and in particular, if a smaller voltage is applied to the interface [9]. As seen in Fig. 3, *therefore, the resistivity of the Cu@MWCNT network, which is lower than the c-axis resistivity of graphite, is related to the filling of Cu into the nano-tubes.*

Finally, the resistivity of the Cu@MWCNT network is also dependent on the number of conductive paths through the network and the number of inter-tube junctions encountered on a given path. Higher density of the network results in the lowering of the resistivity as shown in Fig. 4. Filling Cu into the hollow tubes can only decrease the *intra-tube* resistivity by increasing the conducting cross-section of the tubes.

4. Conclusion

In summary, the Cu@MWCNT network was prepared and its resistivity was measured as a function of temperature and density of the network. The resistivity can be lower than the c-axis resistivity of graphite and has a smaller and constant temperature coefficient over the temperature range from 20 to 500 K. The resistivity decreases with increasing the Cu amount encapsulated into the tubes as well as the density of the network.

Acknowledgments

This work was partially supported by project No. 15-B01, Program of Research for the Promotion of Technological Seeds, Japan Science and Technology Agency. The work was also partially supported by Grant-in-Aid for Exploratory Research No:23651115, Japan Society for the Promotion of Science (JSPS).

References

[1] Bandaru Prabhakar R. J. Nanosci. & Nanotech. 2007; 7: 1239−1267.

[2] Wu ZC, Chen ZH, Du X, Logan JM, Sippel J, Nikolou M, Kamaras K, Reynolds JR, Tanner DB, Hebard AF, Rinzler AG. Science 2004; 305: 1273−1276.

[3] Bekyarova E, Itkis ME, Cabrera N, Zhao B, Yu A, Gao J, Haddon RC. J. Am. Chem. Soc. 2005; 127: 5990−5995.

[4] Bourlon B, Miko C, Forró L, Glattli DC, Bachtold A. Phys. Rev. Lett. 2004; 93: 176806(1−4).

[5] Li HJ, Lu WG, Li JJ, Bai XD, Gu CZ. Phys. Rev. Lett. 2005; 95: 086601(1−4).

[6] Heer WA, Bacsa WS, Chatelain A, Gerfin T, Humphrey-Baker R, Forro L, Ugarte D. Science 1995; 268: 845−847.

[7] Uher C, Hockey RL, Ben-Jacob E. Phys. Rev. B 1987; 35: 4483−4488.

[8] Rochefort A, Avouris P, Lesage F, Salahub DR. Phys. Rev. B 1999; 60: 13824−13830.

[9] Ngo Q, Petranovic D, Krishana S, Cassell AM, Ye Q, Li J, Meyyappan M, Yang CY. IEEE Trans. Nanotech. 2004; 3: 311−317.

[10] Gartland PO, Berge S, Slagsvold BJ. Phys. Rev. Lett. 1972; 28: 738−739.

Figure captions

Fig. 1 (a) Typical SEM image of the Cu@MWCNT pellet, (b) TEM image of the Cu@MWCNT network, and electron beam diffraction patterns of: (c) filled tube and (d) a particle.

Fig. 2 XRD patterns of the Cu@MWCNT powders exposed to air for (a) one week and (b) nine weeks.

Fig. 3 Temperature dependences of the resistivities of the Cu-filled and pristine MWCNT pellets prepared by applying pressure of 128 MPa during heating and cooling. The upper and bottom curves are related to the pellets with the C/Cu ratios of 0.73 and 0.57, respectively. *The curves in the middle shows temperature dependences of the resistivities of the pristine MWCNT pellet, corresponding to the right y-axis.*

Fig. 4 Room-temperature resistivity of the Cu@MWCNT pellets with the C/Cu ratio of 0.57 as a function of the pressure applied during pellet preparation.

Figure 1

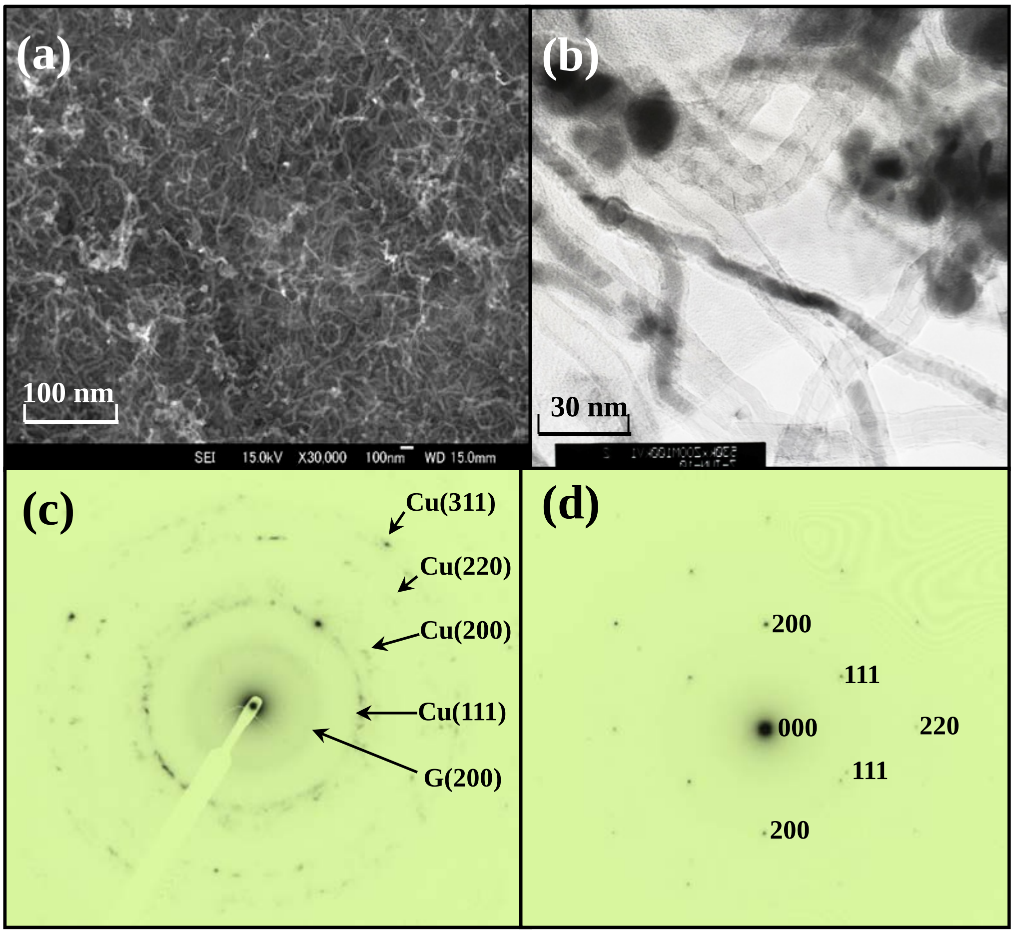

(a)
100 nm
SEI 15.0kV X30,000 100nm WD 15.0mm
(b)
30 nm
(c)
Cu(311)
Cu(220)
Cu(200)
Cu(111)
G(200)
(d)
200
111
000
220
111
200

Figure 2

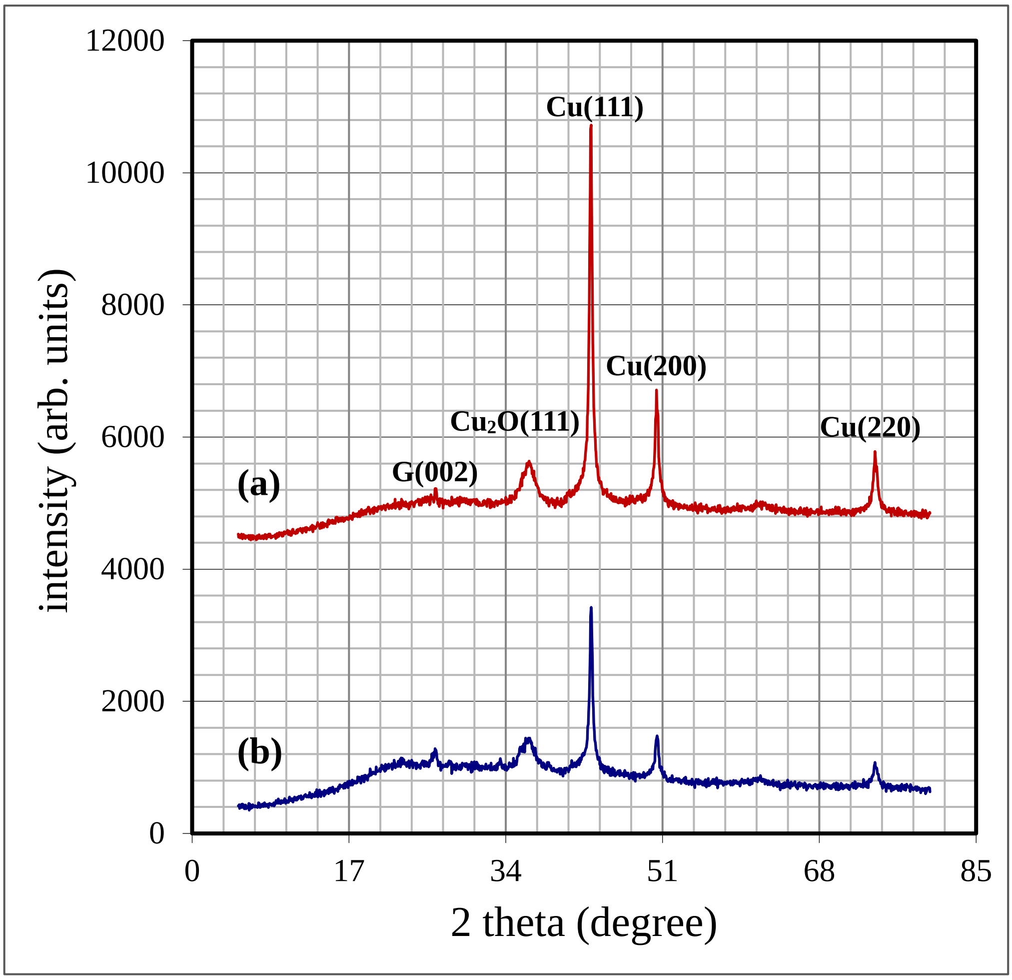

12000
10000
8000
6000
4000
2000
0
intensity (arb. units)
Cu(111)
Cu(200)
Cu2O(111)
Cu(220)
G(002)
(a)
(b)
0
17
34
51
68
85
2 theta (degree)

Figure 3

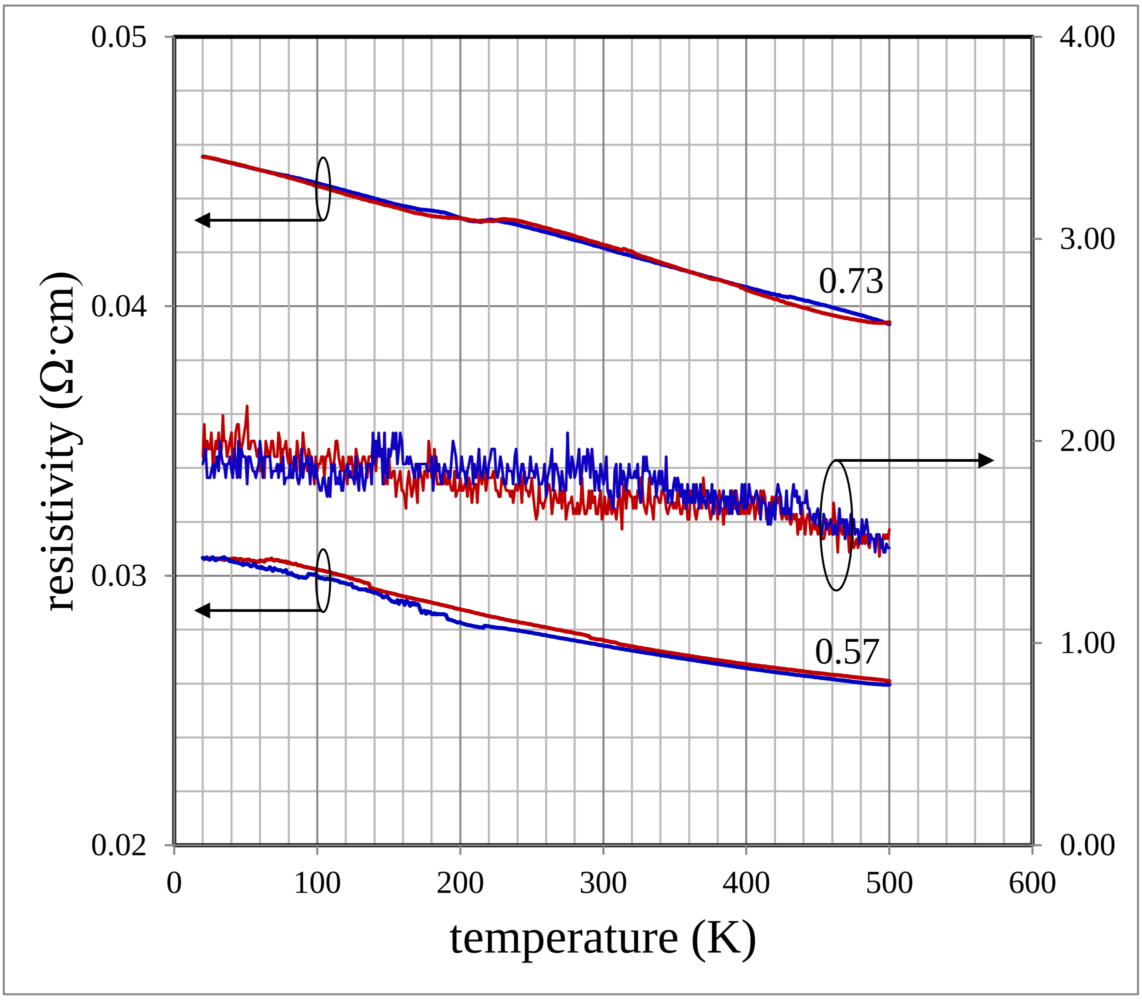

0.05
0.04
0.03
0.02
4.00
3.00
2.00
1.00
0.00
0
100
200
300
400
500
600
resistivity (Ω·cm)
temperature (K)
0.73
0.57

Figure 4

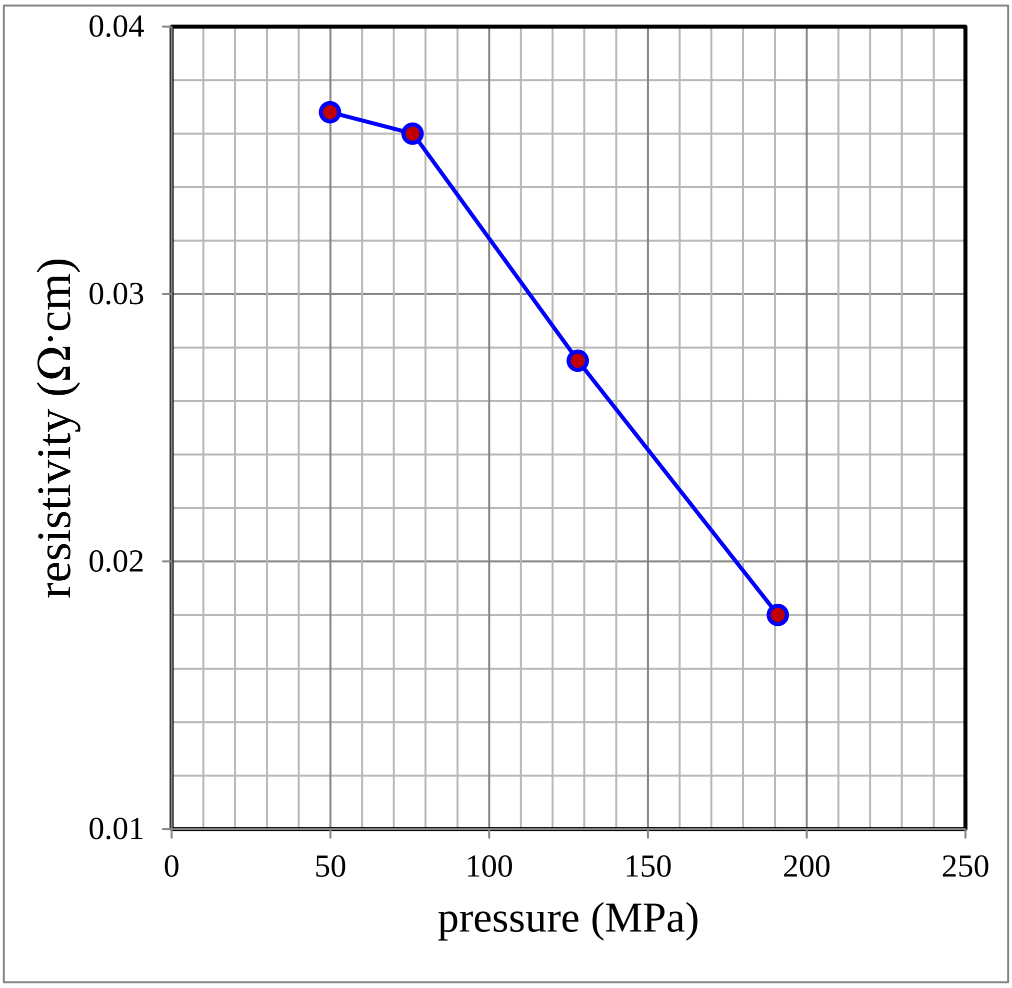

0.04
0.03
0.02
0.01
resistivity (Ω·cm)
0
50
100
150
200
250
pressure (MPa)